



Real time monitoring of glucose in whole blood by smartphone

Miguel M. Erenas^{a,b,*}, Belén Carrillo-Aguilera^a, Kevin Cantrell^c, Sara Gonzalez-Chocano^a, Isabel Maria Perez de Vargas-Sansalvador^{a,b}, Ignacio de Orbe-Payá^{a,b}, Luis Fermin Capitan-Vallvey^{a,b}

^a ECsens., Department of Analytical Chemistry, Faculty of Science, Campus Fuentenueva, University of Granada, 18071, Spain

^b Unit of Excellence in Chemistry applied to Biomedicine and the Environment of the University of Granada, Faculty of Sciences, Campus Fuentenueva, University of Granada, 18071, Spain

^c Department of Chemistry, The University of Portland, 5000 N Willamette Blvd, Portland, OR, 97203, USA



ARTICLE INFO

Keywords:

Thread-paper microfluidic device
Glucose determination
Whole blood
Reaction rate
Smartphone

ABSTRACT

A combined thread-paper microfluidic device (μ TPAD) is presented for the determination of glucose in blood. The device is designed to include all the analytical operations needed: red blood cell separation, conditioning, enzymatic recognition, and colorimetric transduction. The signal is captured with a smartphone or tablet working in video mode and processed by custom Android-based software in real-time. The automatic detection of the region of interest on the thread allows for the use of either initial rate or equilibrium signal as analytical parameters. The time needed for analysis is 12 s using initial rate, and 100 s using the equilibrium measurement with a LOD of 48 μ M and 12 μ M, respectively, and a precision around 7%. The μ TPAD allows a rapid determination of glucose in real samples using only 3 μ L of whole blood.

1. Introduction

In our global society there is a drive to move the acquisition of chemical information from the controlled environments of labs to the place where the information is needed. This necessitates changing the methods used to generate analytical information from approaches that are instrument and lab centered, to decentralized user-centered approaches, the so-called distributed approaches (Hoekstra et al., 2018). One type of analytical system that has the potential to provide fast, laboratory-quality results is lab-on-a-chip devices that rely on microfluidic platforms allowing the miniaturization of chemical assays (Mark et al., 2010). The use of capillarity as a liquid propulsion principle presents advantages over other more complex propulsion systems in terms of simplicity, low cost, biocompatibility, fast response, and user-friendly format. The development of devices based mainly on paper, thread, and cloth have evolved into an active research field with an increasing number of publications and reviews (Akyazi et al., 2018; Aydindogan et al., 2018; Farajikhah et al., 2019; Hoekstra et al., 2018; Li and Steckl, 2018).

In combination with consumer electronic devices that include color sensors, mainly smartphones and tablets, capillary-based devices have the potential to become a total analytical system. These total analytical systems must be considered as a whole and include everything needed

to perform the analysis: sampling, sample treatment, conditioning, analyte recognition, measurements, electronic equipment, and data processing. They should operate in the most robust and simple way possible. These systems do not produce data, but information relevant to the user in an understandable format.

The use of thread brings various advantages for the manufacture of analytical devices in terms of definition of path, strength, varied materials, and small volume of samples (Nilghaz et al., 2013). Thread has been used as support for the manufacture of microfluidic devices (μ TAD) that can implement various analytical operations, such as support for recognition (Wu et al., 2016) and transduction reactions (Liu et al., 2017), immobilization of reagents (Galpotheniya et al., 2014), chromatographic (Agustini et al., 2018) or electrophoretic (Cabot et al., 2018) separations, control and manipulation of flow (Ballerini et al., 2011; Li et al., 2018) or sample conditioning (Ulum et al., 2016). The measurement techniques are mainly optical and electrochemical, by integrating electrodes onto the thread (Malon et al., 2017). The most commonly used optical measurements, apart from the visual ones, are based on the acquisition of images from the device with a scanner (Mao et al., 2015) or with a smartphone (Erenas et al., 2016) and subsequent processing.

A variant in the design of microfluidic devices consists of the combination of thread and paper which gives rise to the so-called

* Corresponding author. ECsens., Department of Analytical Chemistry, Faculty of Science, Campus Fuentenueva, University of Granada, 18071, Spain.
E-mail address: erenas@ugr.es (M.M. Erenas).

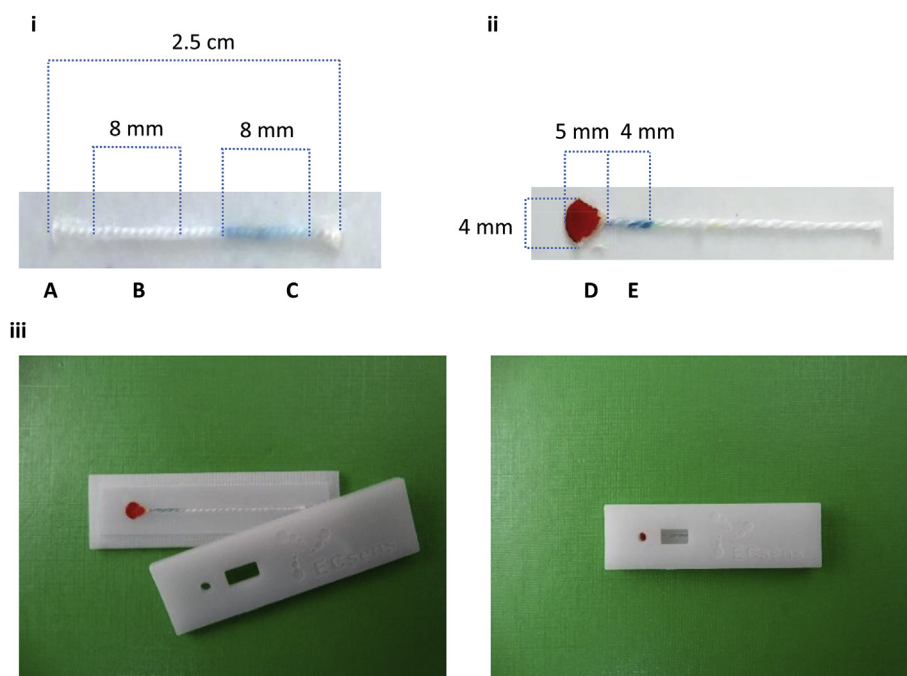


Fig. 1. i) Picture of the μ TAD for glucose: A) Sampling region; B) detection region; C) transduction region. ii) Picture of μ TPAD for whole blood glucose: D) RBC paper based separation membrane and sampling area; E) detection and transduction area. iii) Case designed to contain the μ TPAD with a hole for blood sampling and a window for video recording.

microfluidic thread-paper based analytical device (μ TPAD). These devices developed mainly by the team of Prof. F.A. Gómez, combine the good conduction of fluids by the thread with the recognition process and the subsequent acquisition of the color information from an image of a paper area obtained with a scanner. They have been used for the enzymatic determination of glucose using a three-channel system made with nylon thread and three reaction areas of chromatographic paper (Gonzalez et al., 2016; Lee et al., 2018). Other systems described include a 3D multilayered paper μ TPAD for the determination of glucose and BSA (Neris et al., 2019) and two ELISA for biotinylated goat anti-mouse IgG and rabbit IgG (Gonzalez et al., 2018a, 2018b). Sateanchok et al. (2018) describes a μ TPAD together with a smartphone for the total phenolic content in green tea using a thread portion for the handling of samples and a paper portion for reaction with immobilized reagents.

In this paper we consider the acquisition of the color information of the microfluidic device through a smartphone working in video mode. This opens the door to use kinetic measures to obtain analytical information, which can significantly shorten the analysis time. Additionally, the determination of glucose in whole blood requires separating the red blood cell (RBC) from the plasma, which is achieved with an μ TPAD incorporating a separation membrane. Blood samples collected from volunteers were analyzed with μ TPAD as well as with a portable glucose meter, in order to validate results.

2. Experimental methods

2.1. Materials and equipment

The thread used as support for the μ TPAD preparation was a commercial white cotton thread (caliber 12 and NTex 94) from Finca (Presencia Hilaturas S.A. Alzira, Valencia, Spain) measuring around 600 μ m in diameter and containing 250 ± 10 fibers (Erenas et al., 2016). The reagents included on the thread were 3,3',5,5'-tetramethylbenzidine (TMB), glucose oxidase from *Aspergillus Niger* (GOx), horseradish peroxidase (HRP), chitosan, β -D-glucose, and phosphate buffer solution (1xPBS) containing NaCl, KCl, Na_2HPO_4 and KH_2PO_4 . All these reagents were purchased from Sigma Aldrich (Sigma – Aldrich Quimica S.A., Madrid, Spain). Acetic acid, ethanol, and hydrogen peroxide were purchased from Panreac S.A. (Barcelona, Spain). Reverse osmosis type quality water (Milli-RO 12 plus Milli-Q station (Millipore,

Bedford, MA, U.S.), conductivity 18.2 $\text{M}\Omega$ cm) was used throughout. Whole blood separation membranes MF1, LF1, VF2 and GF/DVA were used and purchased from Whatman (Little Chalfont, Buckinghamshire, United Kingdom).

All the blood samples were obtained from healthy volunteers and collected in tubes containing EDTA to avoid the clotting of samples. Once the blood samples were extracted they were preserved at 4 °C for up to one week.

The μ TAD images were recorded and processed using a variety of devices including a Sony DSC-HX300 digital camera (Sony, Tokyo, Japan), a Samsung Galaxy S5 smartphone, a Samsung Galaxy Tab A tablet (Samsung Electronics, Suwon, South Korea), and a Motorola Moto G4 Play smartphone (Lenovo Goup LTD, Beijing, China). ImageJ software (National Institutes of Health, Bethesda, Maryland, USA) with the Color Space Converter plugin (<http://rsb.info.nih.gov/ij/plugins/color-space-converter.html>) was used to analyze digital images. Avidemux 2.6 (Mean) was used to obtain single frames from video files for analysis by ImageJ. The Anaconda distribution of Python (Continuum Analytics), OpenCV (Open Source Computer Vision), and Android Studio (Google) were used for the development of application software for the processing of video files and for the real-time Android app.

The laboratory evaluations of glucose μ TAD in whole blood and plasma samples were completed for validation purposes using an Accu-Chek Aviva Nano glucose meter (Roche, Switzerland) provided with test-strips.

2.2. Thread-based device preparation

The outer waxy layer of cotton thread, called cuticle, confers hydrophobic properties which affects the wicking and wetting properties. To remove this layer, the thread is scoured in a boiling solution of 10 mg/mL Na_2CO_3 for 5 min (Nilghez and Shen, 2015). Afterwards, the thread is washed several times until the rinsate has a neutral pH, sonicated 3 times in purified water for 5 min, allowed to dry at room temperature, and stored in a closed container for further use.

The basic design of the μ TAD for glucose determination is shown in Fig. 1i. It consists of a 2.5 cm-long thread attached to a piece of double-sided adhesive tape with three different regions: A) a sampling region where sample is placed; B) a recognition region where GOx is retained

and H_2O_2 produced; and C) a transduction region where TMB is oxidized changing the color of thread (Scheme S2). To prepare the device, 5.0 μL of 1xPBS is added in the sampling region and allowed to dry for 2 min. Then 1.0 μL of 1.74 U/ μL GOx is added in the recognition region followed by 0.35 μL of 20.8 mM TMB in ethanol, 0.35 μL of $3.5 \cdot 10^{-2}$ U/mL HRP, and, after waiting 1 min, 0.7 μL of a 1 mg/mL chitosan aqueous solution is added to the transduction region. The device is then left to dry at room temperature for a few minutes. The devices are kept in the darkness until use.

For whole blood glucose determination, the μTAD preparation was modified for the small volume of serum produced (Fig. 1ii). To a 1.5 cm-long piece of thread 2.5 μL of 1xPBS is added to the sampling region and allowed to dry at room temperature for 10 min. Then 0.5 μL of a solution containing $2.8 \cdot 10^{-2}$ U/mL HRP, 3.48 U/mL GOx, 0.5 μL of 14.56 mM TMB in ethanol, and 0.7 μL of 1 mg/mL chitosan in water is deposited in the recognition and transduction region. Finally, a 4 mm \times 5 mm diameter tear-shaped piece of LF1 whole blood separation membrane was placed at the beginning of sampling region of thread.

In order to use the μTAD for whole blood glucose determination we designed a two-piece methacrylate custom case (Fig. 1iii) that holds the thread in a channel engraved for this purpose and allows the acquisition of video with the smartphone. The case was designed using Illustrator software and engraved using a Rayjet Trotec Laser engraving printer (Trotec, Austria) using Rayjet Commander software. A thread and separation membrane are placed on the groove in the bottom piece, and the top, that has two holes for sampling and recording the video, is placed over it, and the μTAD is ready for use.

2.3. μTAD image capture and processing

The digital images were captured using a Sony DSC-HX300 digital camera and Motorola Moto G⁴ Play smartphone. For still images the camera was set-up as follows: resolution of 3648×2736 pixels, aperture value $f/3.5$, exposure time 1/40 s, ISO-80, 2800K white balance (see Fig. S1), and images were saved in jpg format (Joint Photographic Experts Group). For video recordings the camera was set-up as follows: resolution of 1440×1080 pixels, 25 frames per second, and 2800K white balance, and the files were saved in MTS (AVCHD) format. All the images and videos were captured inside a custom cubic light box illuminated by two LED light bulbs (3000K) located in a fixed position. Image and video files from the μTAD were analyzed using ImageJ and the in-house app. All the optimization related to the μTAD and μTPAD , was performed using the Sony digital camera to image the device. Calibration and validation of the device was performed using Motorola Moto G⁴ Play smartphone and the custom Android app.

2.4. Developed software for image-processing

The basic steps employed in the custom image processing software are outlined here, and a more detailed description is given in the supplementary information. The image is first transformed from the RGB color space to the HSV color space. The hue channel is used to identify the type of pixel (e.g. red pixels are whole blood; blue pixels are chemically active areas of the thread), and the saturation channel is used to identify the region of interest and track the degree of color development. An additional set of values, the color absorbance ratios, are also calculated. These three values, hereafter referred to as cA123, are defined as the negative log of the ratio of two RGB channels. For example, cA1 is the $-\log(\text{Blue}/\text{Green})$ (Cantrell et al., 2010). A single region of interest (ROI) was automatically identified as the largest contiguous group of colored pixels. Pixels are masked as colored if their saturation is greater than a threshold amount (≥ 40 in an 8-bit image). Only pixels inside this ROI are used in subsequent data manipulations. For pixels in the ROI, the mean, median, and standard deviation are calculated for RGB, HSV, and cA123, and a histogram of the individual values is

displayed on the screen and recorded in a text file along with the elapsed time for that frame. A subset of the data from 12 s before the elapsed time up to and including the current frame is defined. A least-squares linear fit to the analytical parameter versus time within the 12s window is then calculated. The slope of this line is taken to be the rate of change in the device response. Both the moving average of the analytical parameter and the rate of change are displayed as separate auto-scaling plots. The raw video, processed video, and summary data for each frame are each stored as separate files. The Android-based application was developed and tested using two different Samsung devices. The final calibration and validation of the μTPAD was done with a lower processing capacity Motorola Moto G⁴ Play smartphone.

2.5. Calibration and validation of μTAD and μTPAD

In order to use the μTPAD , 3 μL of whole blood sample was deposited on the sampling area, and a Motorola Moto G⁴ Play smartphone running the Android-based app was used to monitor the color change. To validate the results, the concentrations obtained were compared to a commercial glucometer (Accu-Check) together with the glucose test strips. The test-strip is introduced in the glucometer, and 0.6 μL of whole blood is placed on the sampling area to measure the glucose concentration with the glucometer. Each whole blood sample was analyzed 3 times using the glucometer and results obtained compared to the provided by the μTPAD in terms of percent error.

3. Results and discussion

Thread is a potential substrate for microfluidic devices fabrication with some advantages compared to paper such as high mechanical strength (both in dry and wet conditions), flexibility, lightweight, and ease of functionalization. A large variety of materials with different properties are available, and the thread itself is the driving channel, contrary to what happens in paper in which the channel must be defined (Malon et al., 2017; Nilghaz et al., 2013). A very common substrate is cotton, a super-hydrophilic material, whose specific properties depend on chemical composition and surface morphology (Darmanin and Guittard, 2014). In this application, the gaps intra-yarn, inter-yarn, and lumen of each fiber account for the capillary action by wicking the liquid into the thread (Banerjee et al., 2013). We selected commercial cotton thread ($\sim 600 \mu\text{m}$ diameter and 250 ± 10 fibers) as the material for the capillary platform combined with paper to implement all analytical operations: particles separation, fluid transport, chemistry immobilization and colorimetric transduction. The capillary movement of water in the selected thread shows minor deviation from Washburn-type behavior ($L = a\sqrt{t}$; $a = 0.8185 \pm 0.0065$). The μTAD designed for glucose determination is a single-channel device with a sampling area on one end of the thread and a detection area containing the recognition chemistry at the other end. The principle of the dry-reagent cotton thread-based assay is based on enzymatic oxidation of glucose using GOx/HRP and colorimetric transduction with TMB.

3.1. μTAD optimization

To adjust the enzymatic solution method to the μTAD format, different variables were studied and optimized (additional details are given in the supplementary information). For the transduction reactions the on-thread TMB immobilization, the amount of TMB and HRP, and the pH adjustment were all optimized. For the recognition reactions the amount of GOx and volume of sample added were studied. TMB is the reagent selected for the optical transduction of the enzymatically generated H_2O_2 . TMB is insoluble in water, but the blue oxidation product is soluble and can be dragged through the medium by the sample. Chitosan is used to preconcentrate the oxidized TMB in the detection area as it is strongly retained to paper (Ariza-Avidad et al., 2016; Gabriel et al., 2016) and cloth-based devices (Bagherbaigi et al., 2014).

It slows the movement of the oxidized TMB and increases the homogeneity of the ROI (Liu et al., 2014). The deposition of 0.7 μg of chitosan (0.7 μl of 1 mg/mL solution) reduces the length of TMB oxidized area (16%) and improves reproducibility (from 20.3% CV without chitosan to 3.6% with it, $n = 3$) (Table S1).

As TMB and HRP mutually influence one another, their optimization was performed simultaneously by a factorial design obtaining a maximum saturation signal for 14.0 μU and $7.3 \cdot 10^{-3}$ μmol of HRP and TMB, respectively (Fig. S3). The immobilization by drying of pH 7.4 PBS buffer in the thread improves the precision (7.6% compared to 11.5%) and simplifies the use of the device, thus we included the buffer in the μTAD although it reduces the equilibrium value of the saturation signal (Fig. S4).

To study the GOx dependence, different concentrations were deposited on the thread and the evolution of saturation signal was monitored over time (Fig. S5). The largest saturations were obtained with 1.74 U of GOx. Interestingly a substantial lowering in the reaction time for equilibration (100 s) was observed, which is a much lower time than described in literature, typically around 10 min (Table S3).

The maximum saturation signal was obtained for 10 μL samples. For smaller volumes, the signal decreases because a smaller amount of glucose is present, and the precision is lower due to the thread not being completely wet (Fig. S6). Alternatively, at higher sample volumes the oxidized TMB is dragged from ROI, decreasing the signal and lowering the precision.

3.2. μTAD analytical characterization

To study the performance of the system we prepared 10 different glucose standards, five replicates each, using 50 different μTAD devices (each is a one-use device) while recording the evolution of colors with a smartphone in real-time using the custom Android app. As analytical parameters we studied both the initial reaction rate using a window of 12 s from the time when the app detects a change on the color of thread (Fig. 2) and the equilibrium signal measured as the saturation 100 s after the sample addition (Fig. S7). In both cases, the relationship between the logarithm of glucose concentration and the analytical parameter is sigmoidal and is fitted to a Boltzmann equation (Equation (1)).

$$y = A_2 + \frac{(A_1 - A_2)}{1 + e^{\frac{(x-A_3)}{A_4}}} \quad (1)$$

Analytical figures of merit obtained using both methods (rate based and equilibrium) are shown in Table 1. The limit of detection was calculated as 6 times the standard deviation of the blank (Mistberger et al., 2014), obtaining a value of 48 μM for initial rate and 12 μM when equilibrium saturation is used. These values are much lower than those in the literature for colorimetric μPAD 's for glucose (Chun et al., 2014; Gabriel et al., 2017; Gonzalez et al., 2016) and comparable to those

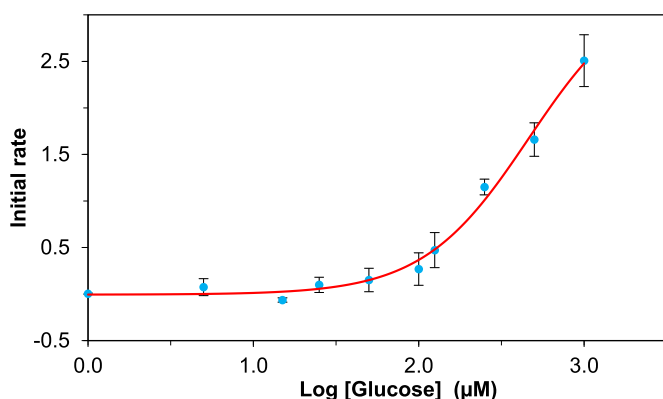


Fig. 2. Calibration of μTAD sensing membrane using initial rate and adjust to a Boltzmann equation.

Table 1

Calibration function and analytical parameter of the method when saturation and initial rate are used as analytical parameter.

Calibration function (Initial rate)		Calibration function (Saturation)		Calibration function (Total blood)	
A1	-0.006	A1	0.164	Intercept	5.344
A2	3.352	A2	0.776	Slope	0.257
A3	2.666	A3	2.403	R^2	0.991
A4	0.320	A4	0.490	LOD	28 mg/dL
R^2	0.987	R2	0.966	Analysis time	~ 10 s
LOD	48 μM	LOD	12 μM		
Analysis time	12 s	Analysis time	100 s		

Precision (n = 10)					
15 μM	10.2%	15 μM	7.8%	50 mg/dL	6.6%
125 μM	5.7%	125 μM	7.2%	90 mg/dL	6.9%
500 μM	9.1%	500 μM	5.5%	110 mg/dL	5.2%

obtained by a bipolar ECL thread-based method (Liu et al., 2017) (Table S3). A precision study was also performed at three different concentrations, 10 replicates each, obtaining values ranging from 5.5% to 7.8%. Although an analysis time of 100 s is a major improvement for colorimetric devices compared with literature (Ariza-Avidad et al., 2016; Gabriel et al., 2017; Zhu et al., 2017), the use of initial rate measured in real-time further reduces the analysis time down to 12 s. A study of the stability of μTAD over time in two different preservation conditions, fridge and desiccator, showed short lifetimes (Fig. S8) as is typical for these systems (Zhu et al., 2017).

3.3. Glucose determination in whole blood

To perform the conventional spectrophotometric determination of glucose in blood in the laboratory, it is necessary to separate plasma from the RBC via centrifugation, to avoid their interference in the blue color of oxidized TMB (Li and Steckl, 2018). In order to meet the AS-SURED guidelines (Mabey et al., 2004), we studied the inclusion of an RBC separation step in the developed μTAD while keeping the device as small as possible.

Different strategies have been described in literature to integrate RBC separation from plasma in paper and thread devices. Some are based on the use of different salts in the thread to induce blood clotting, such as NaCl (Nilghaz and Shen, 2015; Yan et al., 2014) or CaCl_2 (Li et al., 2014); anticoagulants such as EDTA (Ulum et al., 2016); agglutinating antibodies (Al-Tamimi et al., 2012; Yang and Lin, 2015) or paper membranes (Songjaroen et al., 2012).

The use of NaCl or EDTA in different conditions of concentration and temperature did not result in appreciable separation of plasma in the small volumes of blood used (see SI 3.8). Blood filter paper (Songjaroen et al., 2012) is used to separate the RBC from whole blood by trapping them on the membrane while allowing plasma to flow by capillarity to the recognition area. As paper filters to remove particles greater than 2–3 μm , we tested polyvinyl alcohol-bound glass fiber membranes (MF1, LF1 and VF2) and binder-free glass fiber membrane (VF1). To test filter papers, a 6 mm round shape membrane was located at the beginning of the μTAD and 10 μL of whole blood was used. Only LF1 paper provided a sufficient amount of plasma for samples this small.

To reduce the blood volume needed, we designed a tear shape membrane connected to the thread by the tip (Fig. 1ii) and tested different tear sizes and blood volumes. We selected a 4 mm \times 5 mm diameter tear-shaped membrane and 3 μL of blood. Fig. 3 shows the plot-line saturation profiles of the device with 3 μL and 4 μL of blood. A sharp change in saturation is observed for the 3 μL sample size indicating better RBC separation than the progressive increase seen in the 4 μL sample size.

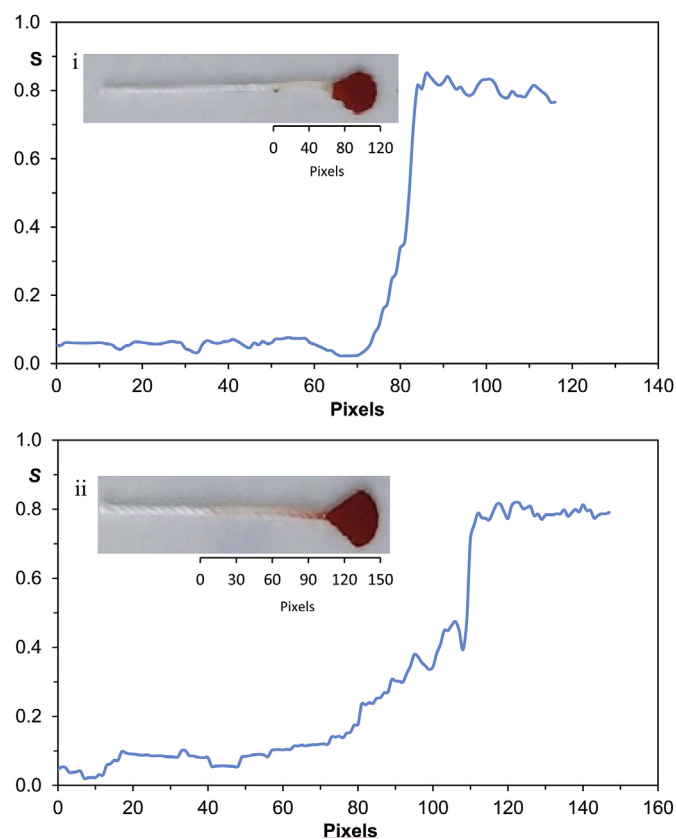


Fig. 3. Saturation (S) plot profile of the device when different volumes of 3 and 4 μL of whole blood sample are added. i) 3 μL ; ii) 4 μL .

Due to the low volume of plasma obtained from 3 μL of whole blood, it was necessary to redesign the device to overlap the recognition and detection areas (Fig. 1ii). Consequently, we designed a combined thread – paper microfluidic device, a μTPAD , to include the different analytical operations needed for glucose analysis in total blood: RBC separation, conditioning, recognition, and transduction.

For ease the use, we designed a custom casing in two-piece methacrylate. The bottom is engraved with a slit that allows lodging both the thread and the membrane in a fixed position. The top has two holes for sampling and collecting the signal with the smartphone (Fig. S4). This housing was designed to fulfill the ASSURED guidelines of user-friendly operation and safety; the user cannot touch the sampling area or thread where the reaction will occur.

To calibrate the μTPAD a series of whole blood samples with known amounts of glucose around physiological levels were prepared. A 50 μL aliquot of whole blood was left at room temperature for 6 h so that glycolysis consumes the glucose present, and it was then spiked with 0.5 μL of a glucose standard. The calibration function is shown in Fig. 4, and the details of the fit to linear equation and figures of merit are presented in Table 1. Due to the rapid change in color of the μTPAD when a whole blood sample is analyzed, it is not possible to use the initial rate as analytical parameter.

A precision study was carried out at 50.0, 90.0 and 110.0 mg/dL of glucose, with 10 replicates per solution. Relative standard deviations of 6.6%, 6.9% and 5.2%, respectively, were measured. Taking into account that the precision of the colorimetric method in a laboratory is around 5% (Burtis et al., 2008), the values obtained with this device are quite acceptable. This complete system not only measures the glucose concentration, but it also separates plasma from whole blood and performs multiple buffered reactions without any manipulation of sample. Finally, the price of a sensor was estimated to be 0.0087 €/ μTPAD without the case and 0.0999 €/ μTPAD including it. (Table S2).

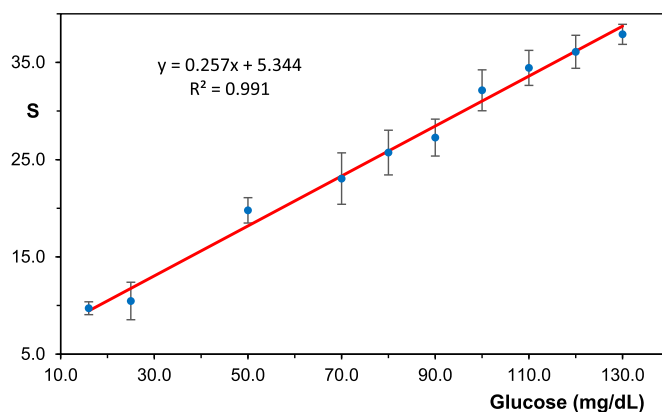


Fig. 4. Calibration ($n = 5$) of μTPAD obtained from whole blood spiked samples using saturation (S) as analytical parameter.

Once the development and optimization of the different variables were performed, a study of interference species was carried out (Section 3.1 in the SI) and finally, the μTPAD was applied to real whole blood samples supplied from seven different healthy volunteers. In all cases, 3 μL of blood was added to the μTAD without any kind of previous treatment. The measured values range from 3% to 17% (Table 2) percent error when compared to a commercial glucose meter.

4. Conclusions

This study develops the first colorimetric microfluidic-based procedure combined with a smartphone app to obtain kinetic or equilibrium signals in real time. The procedure is implemented in a microfluidic single-channel device that combines cotton thread and paper, μTPAD , for glucose analysis in whole blood with no need for any pre-treatment. The combination of several analytical operations, such as buffering, and the separation of the red blood cells from the plasma, along with the use of thread as the support simplifies the operational procedure and reduces the analysis time. The analytical approach shown here can be extended to the real-time monitoring of a variety of chemicals or biomarkers by selecting the type of procedure (kinetic/equilibrium), depending on the concentration of the analyte in combination with capillary microfluidic devices. This strategy opens the way to the simple application of kinetic procedures using a smartphone, increasing the versatility of ready-to-use procedures.

The main limitation of the presented procedure is related to the short lifetime of the μTPAD device, due to the loss of activity of the enzymatic material. Future work will focus on replacing enzymes with nanozymes or including enzymes in co-embedded flower-like nanomaterials to improve the lifetime of the device, as well as developing kinetic procedures for on-site detection based on processing information captured with a smartphone video camera and thread-based devices.

Table 2

Validation of whole blood samples using the μTPAD and a commercial glucose meter as reference method.

Whole blood sample	Glucose meter	μTPAD	Error
1	65 mg/dL	67 mg/dL	3%
2	66 mg/dL	72 mg/dL	10%
3	51 mg/dL	60 mg/dL	17%
4	65 mg/dL	59 mg/dL	10%
5	73 mg/dL	75 mg/dL	3%
6	119 mg/dL	113 mg/dL	5%
7	67 mg/dL	79 mg/dL	4%

Declaration of interests

The authors declare that they have no known competing financial interests or personal relationships that could have appeared to influence the work reported in this paper.

CRedit authorship contribution statement

Miguel M. Erenas: Conceptualization, Formal analysis, Methodology, Supervision, Writing - original draft. **Belén Carrillo-Aguilera:** Methodology, Investigation. **Kevin Cantrell:** Software, Formal analysis, Writing - original draft. **Sara Gonzalez-Chocano:** Investigation, Visualization. **Isabel Maria Perez de Vargas-Sansalvador:** Formal analysis, Methodology. **Ignacio de Orbe-Payá:** Writing - original draft, Visualization. **Luis Fermin Capitan-Vallvey:** Conceptualization, Resources, Supervision, Writing - original draft, Funding acquisition.

Acknowledgements

This study was supported by the CTQ2016-78754-C2-1-R project from the Spanish MINECO.

Appendix A. Supplementary data

Supplementary data to this article can be found online at <https://doi.org/10.1016/j.bios.2019.04.024>.

References

- Agustini, D., Fedalto, L., Bergamini, M.F., Marcolino-Junior, L.H., 2018. *Lab Chip* 18, 670–678.
- Akyazi, T., Basabe-Desmonts, L., Benito-Lopez, F., 2018. *Anal. Chim. Acta* 1001, 1–17.
- Al-Tamimi, M., Shen, W., Zeineddine, R., Tran, H., Garnier, G., 2012. *Anal. Chem.* 84, 1661–1668.
- Ariza-Avidad, M., Salinas-Castillo, A., Capitan-Vallvey, L.F., 2016. *Biosens. Bioelectron.* 77, 51–55.
- Aydindogan, E., Guler Celik, E., Timur, S., 2018. *Anal. Chem.* 90, 12325–12333.
- Bagherbaigi, S., Corcoles, E.P., Wicaksono, D.H.B., 2014. *Anal. Methods* 6, 7175–7180.
- Ballerini, D.R., Li, X., Shen, W., 2011. *Biomicrofluidics* 5, 014105-1-014105/13.
- Banerjee, S.S., Roychowdhury, A., Taneja, N., Janrao, R., Khandare, J., Paul, D., 2013. *Sens. Actuators, B* 186, 439–445.
- Burtis, A.C., Edwrd, R., Bruns, E.,D., 2008. *Fundamentals of Clinical Chemistry*, sixth ed. Building. Elsevier.
- Cabot, J.M., Breadmore, M.C., Paull, B., 2018. *Anal. Chim. Acta* 1000, 283–292.
- Cantrell, K., Erenas, M.M., Orbe-Paya, I., Capitan-Vallvey, L.F., 2010. *Anal. Chem.* 82, 531–542.
- Chun, H.J., Park, Y.M., Han, Y.D., Jang, Y.H., Yoon, H.C., 2014. *BioChip J.* 8, 218–226.
- Darmanin, T., Guittard, F., 2014. *Prog. Polym. Sci.* 39, 656–682.
- Erenas, M.M., de Orbe-Paya, I., Capitan-Vallvey, L.F., 2016. *Anal. Chem.* 88, 5331–5337.
- Farajikhah, S., Cabot, J.M., Innis, P.C., Paull, B., Wallace, G.G., 2019. *ACS Comb. Sci.* 21 (4), 229–240.
- Gabriel, E.F.M., Garcia, P.T., Cardoso, T.M.G., Lopes, F.M., Martins, F.T., Coltro, W.K.T., 2016. *Analyst* 141, 4749–4756.
- Gabriel, F.E., Garcia, T.P., Lopes, M.F., Coltro, K.W., 2017. *Micromachines* 8, 104.
- Galpothdeniya, W.I., McCarter, K.S., De Rooy, S.L., Regmi, B.P., Das, S., Hasan, F., Tagge, A., Warner, I.M., 2014. *RSC Adv.* 4, 7225–7234.
- Gonzalez, A., Estala, L., Gaines, M., Gomez, F.A., 2016. *Electrophoresis* 37, 1685–1690.
- Gonzalez, A., Gaines, M., Gallegos, L.Y., Guevara, R., Gomez, F.A., 2018a. *Electrophoresis* 39, 476–484.
- Gonzalez, A., Gaines, M., Gallegos, L.Y., Guevara, R., Gomez, F.A., 2018b. *Methods* 146, 58–65.
- Hoekstra, R., Blondeau, P., Andrade, F.J., 2018. *Anal. Bioanal. Chem.* 410, 4077–4089.
- Lee, W., Gonzalez, A., Arguelles, P., Guevara, R., Gonzalez-Guerrero, M.J., Gomez, F.A., 2018. *Electrophoresis* 39, 1443–1451.
- Li, H., Han, D., Pauletti, G.M., Steckl, A.J., 2014. *Lab Chip* 14, 4035–4041.
- Li, H., Steckl, A.J., 2018. *Anal. Chem.* 91, 352–371.
- Li, Y.D., Li, W.Y., Chai, H.H., Fang, C., Kang, Y.J., Li, C.M., Yu, L., 2018. *Cellulose* 25, 4831–4840.
- Liu, R., Liu, C., Li, H., Liu, M., Wang, D., Zhang, C., 2017. *Biosens. Bioelectron.* 94, 335–343.
- Liu, W., Yang, H., Ding, Y., Ge, S., Yu, J., Yan, M., Song, X., 2014. *Analyst* 139, 251–258.
- Mabey, D., Peeling, R.W., Ustianowski, A., Perkins, M.D., 2004. *Nat. Rev. Microbiol.* 2, 231.
- Malon, R.S.P., Heng, L.Y., Corcoles, E.P., 2017. *Rev. Anal. Chem.* 36, 1–19.
- Mao, X., Du, T.E., Meng, L., Song, T., 2015. *Anal. Chim. Acta* 889, 172–178.
- Mark, D., Haerberle, S., Roth, G., von Stetten, F., Zengerle, R., 2010. *Chem. Soc. Rev.* 39, 1153–1182.
- Mistberger, G., Crespo, G.A., Bakker, E., 2014. *Annu. Rev. Anal. Chem.* 7, 483–512.
- Neris, N.M., Guevara, R.D., Gonzalez, A., Gomez, F.A., 2019. *Electrophoresis* 40, 296–303.
- Nilghaz, A., Ballerini, D.R., Shen, W., 2013. *Biomicrofluidics* 7, 51501.
- Nilghaz, A., Shen, W., 2015. *RSC Adv.* 5, 53172–53179.
- Sateanchok, S., Wangkarn, S., Saenjum, C., Grudpan, K., 2018. *Talanta* 177, 171–175.
- Songjaroen, T., Dunchai, W., Chailapakul, O., Henry, C.S., Laiwattanapaisal, W., 2012. *Lab Chip* 12, 3392–3398.
- Ulum, M.F., Maylina, L., Noviana, D., Wicaksono, D.H.B., 2016. *Lab Chip* 16, 1492–1504.
- Wu, T., Xu, T., Xu, L.P., Huang, Y., Shi, W., Wen, Y., Zhang, X., 2016. *Biosens. Bioelectron.* 86, 951–957.
- Yan, C., Yu, S., Jiang, Y., He, Q., Chen, H., 2014. *Hua Xue Xue Bao* 72, 1099–1104.
- Yang, Y.A., Lin, C.H., 2015. *Biomicrofluidics* 9, 022402-1-022402/12.
- Zhu, X., Huang, J., Liu, J., Zhang, H., Jiang, J., Yu, R., 2017. *Nanoscale* 9, 5658–5663.